



The neuroinflammatory component of negative affect in patients with chronic pain

D. S. Albrecht¹ · M. Kim¹ ¹ · O. Akeju² · A. Torrado-Carvajal¹ ¹ · R. R. Edwards³ · Y. Zhang² · C. Bergan¹ · E. Protsenko¹ · A. Kucyi^{1,4} · A. D. Wasan⁵ · J. M. Hooker¹ · V. Napadow^{1,3} · M. L. Loggia¹

Received: 2 December 2018 / Revised: 5 March 2019 / Accepted: 11 April 2019
© The Author(s), under exclusive licence to Springer Nature Limited 2019

Abstract

Negative affect (NA) is a significant cause of disability for chronic pain patients. While little is known about the mechanism underlying pain-comorbid NA, previous studies have implicated neuroinflammation in the pathophysiology of both depression and chronic pain. Here, we tested the hypothesis that NA in pain patients is linked to elevations in the brain levels of the glial marker 18 kDa translocator protein (TSPO), and changes in functional connectivity. 25 cLBP patients (42.4 ± 13 years old; 13F, 12M) with chronic low back pain (cLBP) and 27 healthy control subjects (48.9 ± 13 years old; 14F, 13M) received an integrated (i.e., simultaneous) positron emission tomography (PET)/magnetic resonance imaging (MRI) brain scan with the second-generation TSPO ligand [¹¹C]PBR28. The relationship between [¹¹C]PBR28 signal and NA was assessed first with regression analyses against Beck Depression Inventory (BDI) scores in patients, and then by comparing cLBP patients with little-to-no, or mild-to-moderate depression against healthy controls. Further, the relationship between PET signal, BDI and frontolimbic functional connectivity was evaluated in patients with mediation models. PET signal was positively associated with BDI scores in patients, and significantly elevated in patients with mild-to-moderate (but not low) depression compared with controls, in anterior middle and pregenual anterior cingulate cortices (aMCC, pgACC). In the pgACC, PET signal was also associated with this region's functional connectivity to the dorsolateral PFC (pgACC-dlPFC), and mediated of the association between pgACC-dlPFC connectivity and BDI. These observations support a role for glial activation in pain-comorbid NA, identifying in neuroinflammation a potential therapeutic target for this condition.

Supplementary information The online version of this article (<https://doi.org/10.1038/s41380-019-0433-1>) contains supplementary material, which is available to authorized users.

✉ M. L. Loggia
marco.loggia@mgh.harvard.edu

- ¹ A.A. Martinos Center for Biomedical Imaging, Massachusetts General Hospital, Harvard Medical School (MGH/HMS), Boston, MA, USA
- ² Department of Anesthesia, Critical Care and Pain Medicine, MGH/HMS, Boston, MA, USA
- ³ Department of Anesthesiology, Perioperative and Pain Medicine, Brigham and Women's Hospital, HMS, Boston, MA, USA
- ⁴ Department of Neurology, Stanford University Medical Center, Stanford, CA, USA
- ⁵ Departments of Anesthesiology and Psychiatry, University of Pittsburgh, Pittsburgh, PA, USA

Introduction

The experience of chronic pain is intimately linked with negative affect (NA), which can significantly complicate presentation, clinical course and treatment response [1]. Indeed, ~40% of chronic low back pain (cLBP) patients, the most common chronic pain disorder, exhibit comorbid NA, including major depression, anxiety, and high levels of pain catastrophizing [2–5]. Patients with comorbid chronic pain and high NA report significantly higher pain severity and interference, and lower quality of life, than individuals with chronic pain or mood disorders alone [6–8].

A growing body of evidence suggests that neuroinflammation is associated with chronic pain and NA, and may in fact be a common substrate contributing to both conditions. For instance, elevated levels of circulating inflammatory markers have been detected in patients with chronic pain and/or depression [9, 10]; preclinical studies demonstrate brain glial activation in models of both chronic pain [11–14] and chronic stress [15–19]; and finally, human

imaging studies provide evidence of central nervous system (CNS) glial activation in chronic pain patients [20–22], as well as patients with depression [23–26] (although see ref. [27]). While these data support a role for glial activation in the pathophysiology of both chronic pain and affective disorders, no study has yet investigated the neuroinflammatory component of depressive symptoms comorbid with chronic pain.

The principal aim of the current study was to test the hypothesis that cLBP with comorbid NA is accompanied by neuroinflammation in frontolimbic and insular cortices [23–25]. We studied cLBP patients with depression scores ranging from low to mild/moderate, as well as healthy, non-depressed controls, using integrated positron emission tomography/magnetic resonance imaging (PET/MRI) and [¹¹C]PBR28. This radioligand binds to the 18-kDa translocator protein (TSPO), a mitochondrial protein that is considered a putative imaging biomarker of neuroinflammation [28] because it is expressed at low levels in healthy CNS tissue [29], but is consistently upregulated in activated microglia and/or astrocytes during neuroinflammatory responses [30].

In addition, a secondary aim was to evaluate the relationship between neuroimmune activation and functional connectivity. This aim is motivated by the potential existence of a bidirectional relationship between glial activation and neural communication, as the former per se is able to modulate synaptic transmission [31], and conversely, neural activity is also able to trigger activation of neuroimmune cells, e.g., in neurogenic neuroinflammation [32]. Given the interplay between neuroinflammation and neural communication, and because aberrant functional connectivity has been documented in patients with chronic pain [33, 34] and in those with depression [35, 36], we tested for the presence of an association between glial activation and functional connectivity as assessed using resting-state blood oxygen level-dependent functional magnetic resonance imaging (BOLD fMRI) data collected simultaneously to the [¹¹C]PBR28 PET signal.

Materials and methods

Subjects

Twenty-five patients diagnosed with cLBP more than 6 months before enrollment, and rating their average pain at least 3/10 during a typical week for at least half the week. In addition, an existing dataset of 27 healthy, pain-free controls was used to perform the (secondary) group analyses. While no formal calculation was performed to specifically estimate the power needed to detect an association between [¹¹C]PBR28 signal and BDI, previous studies have identified a statistically significant correlation between TSPO

signal and measures of negative affect with smaller samples [23, 25], suggesting that we would have sufficient power to detect such an association in our own sample. Data for 10 patients and 9 controls have been previously reported as part of a study not investigating the role of neuroinflammation in negative affect [21]. Exclusion criteria included any PET/MRI contraindications (including pregnancy, metallic implants, claustrophobia), any past or present major medical, neurological, or psychiatric illness (general anxiety disorder, PTSD, and depression were only exclusionary if severe enough to require hospitalization in the past 5 years), or illicit drug use as confirmed by subjective report and urine drug screening. Recruitment took place between 4 April 2012 and 27 November 2017.

All study procedures were performed at the Athinoula A. Martinos Center for Biomedical Imaging at Massachusetts General Hospital. All protocols were approved by the Institutional Review Board and Radioactive Drug Research Committee, and all subjects signed a written informed consent.

Behavioral visit

At the first visit, all subjects underwent a medical history and physical examination, and provided a urine sample was obtained for drug screening. Subjects were genotyped for the Ala147Thr *TSPO* polymorphism, which affects [¹¹C]PBR28 binding to TSPO [37, 38], and were included in the subsequent imaging portion of the study only if they exhibited the ala/ala (“high affinity binders”, HABs) or ala/thr (“mixed affinity binders”, MABs), but not the thr/thr (“low affinity binders”) genotype. Participants also completed the Beck Depression Inventory BDI-1A [39], which has shown good psychometric properties in individuals with chronic pain [40], as well the McGill Pain Questionnaire, short form [41].

Imaging visit

Dynamic [¹¹C]PBR28 PET and structural MR data were acquired for 90 min as described previously [21, 42]. Simultaneously to the PET data, a 6-min blood oxygen level-dependent (BOLD) resting-state fMRI scan was acquired for each subject (TR/TE = 2 s/30 ms, flip angle = 90°, voxel size = 3.1 × 3.1 × 3 mm, 37 slices), with eyes open. All subjects rated their current clinical pain during the scan, using a Numerical Rating Scale from 0 (no pain) to 100 (the most intense pain tolerable).

Data preprocessing

[¹¹C]PBR28 PET data

SUV images, 60–90 min post-injection, normalized by whole brain uptake (SUV_R), were generated as described

previously [21, 42, 43]. Briefly, a 90-min dynamic [^{11}C]PBR28 PET acquisition and MR-imaging were performed with an integrated PET/MRI scanner consisting of a dedicated brain avalanche photodiode-based PET scanner in the bore of a Siemens 3T Tim Trio MRI [44]. [^{11}C]PBR28 was produced in-house using a procedure modified from the literature [45]. A multi-echo MPRAGE volume was acquired prior to tracer injection (TR/TE1/TE2/TE3/TE4 = 2530/1.64/3.5/5.36/7.22 ms, flip angle = 7° , voxel size = 1 mm isotropic) for the purpose of anatomical localization, spatial normalization of the imaging data, as well as generation of attenuation correction maps [46]. MPRAGE-based attenuation correction was performed according to published methods [46]. SUV maps were nonlinearly transformed to MNI space and smoothed with an 8 mm full width at half-maximum Gaussian kernel. Finally, SUV frames were normalized by average whole-brain uptake to obtain SUV ratios (SUVR), as our group has described previously for [^{11}C]PBR28 [21]. This method has been used in several [^{11}C]PBR28 studies, including in cLBP patients, and demonstrates good ability to detect signal elevations in regions where neuroinflammation is known or expected to occur, e.g., motor cortex in amyotrophic lateral sclerosis, basal ganglia in Huntington's disease [21, 43, 47–50]. Importantly, in order to validate the use of SUVR as an outcome metric, we compared SUVR against V_T ratio (DVR) in a subset of subjects for whom arterial plasma data were available. These correlations reached statistical significance for all regions evaluated in this study (a priori ROIs and regions identified in the voxelwise regression analyses; $0.59 \leq r \leq 0.85$, $0.034 \leq p \leq 0.001$), except for the prefrontal ROI, which showed a strong trend ($r = 0.55$; $p = 0.053$; Supplementary Fig. 1). These analyses therefore provided support to the use of SUVR as viable PET metric in our study.

Resting-state fMRI data

Six-minute BOLD scans were pre-processed using FSL (FMRIB's Software Library, <http://www.fmrib.ox.ac.uk/fsl/>), AFNI (<http://afni.nimh.nih.gov/afni>), and FreeSurfer (<http://surfer.nmr.mgh.harvard.edu/>) software packages. Data were corrected for slice-timing, physiological motion, and B0 field inhomogeneities. Brain extraction, co-registration to the MPRAGE, spatial smoothing with a 6-mm Gaussian kernel, high-pass temporal filtering ($f = 0.008$ Hz), and nonlinear transformation to MNI space were subsequently performed. To reduce physiological noise, we employed denoising with a principle component analysis (PCA), aCompCor [51]. In order to reduce physiological noise in the resting-state BOLD data, MPRAGE images were segmented in probabilistic maps of gray matter (GM), white matter (WM), and cerebrospinal fluid (CSF) using SPM 12

(<http://www.fil.ion.ucl.ac.uk/spm/>). To minimize potential partial volume effects, WM and CSF masks were thresholded at 90% and eroded by one voxel. BOLD data were masked with WM and CSF inclusive masks, and a principal component analysis was performed on the masked data. WM and CSF noise time courses were extracted only from unsmoothed functional BOLD data. To determine whether NA-related neuroinflammation was associated with neural communication, we performed seed-based functional connectivity analyses investigating the regions demonstrating the strongest association between [^{11}C]PBR28 signal and BDI scores: the anterior middle and pregenual anterior cingulate cortices (aMCC, pgACC; see the "Results" section). To this end, the average BOLD time series was extracted from 3-mm-radius spheres placed around the peak voxels identified in the voxelwise regression analysis (MNI coordinates, x,y,z [mm]): ($-10,36,22$) and ($2,40,-2$) for the aMCC and pgACC, respectively.

Statistical analysis

To test the relationship between neuroinflammation signal and negative affect we adopted a multi-stage approach. In broad terms, we first identified regions demonstrating a statistically significant association between [^{11}C]PBR28 signal and BDI scores in patients, using both region-of-interest (ROI) and voxelwise regression analyses. The mean [^{11}C]PBR28 signal extracted from the regions identified in the voxelwise regression analyses was then compared between patients, split into subgroups with "mild-to-moderate" or "low-to-none" depression, and a group of healthy non-depressed controls. The purpose of these follow-up group analyses was to further elucidate the link between negative affect and TSPO signal, by specifically testing the hypothesis that only patients with "mild-to-moderate depression" would demonstrate statistically elevated [^{11}C]PBR28 compared with controls (and not patients with levels of NA comparable to those of healthy controls), in those regions.

More in detail, we first performed a partial correlation analysis between BDI scores and [^{11}C]PBR28 SUVR in patients, correcting for *TSPO* genotype, in three anatomically defined ROIs (PFC, insula, and ACC), because a recent study in major depression disorder demonstrated an association between depression scores and *TSPO* level in these regions [25]. Significance was set at $p < 0.05$ (Bonferroni-corrected for multiple comparisons). As a follow-up analysis, the same analysis was run for "control" regions we previously showed to exhibit elevated [^{11}C]PBR28 signal in cLBP patients, but not expected to be related to NA: left and right thalamus (anatomically defined), and a subregion of the left thalamus identified in voxelwise analyses [21]. PFC, insula, and left and right

thalamic ROIs were created from the Harvard-Oxford Cortical Structural Atlas (Centre for Morphometric Analyses, http://www.cma.mgh.harvard.edu/fsl_atlas.html) according to landmarks described in the study, and thresholded at the arbitrary value of 30 as performed previously [21]. Because the Harvard-Oxford label of the ACC contains posterior portions likely belonging to middle and posterior cingulate cortex, the ACC ROI was obtained with Neurosynth [52], using “anterior cingulate cortex” as a term in a reverse inference search, thereby excluding posterior portions of the cingulate cortex present in the Harvard-Oxford label. The left thalamus cluster ROI corresponded to the left thalamic cluster that exhibited statistically significant differences across groups in our previous study [21]. Because the distribution of residuals for the partial correlations comparing SUVR values from all ROIs with BDI scores did not significantly deviate from normality (p 's > 0.076, Shapiro-Wilk), the use of Pearson's correlation was appropriate.

Because a statistically significant association between TSPO PET signal and BDI was either reached (ACC) or approached (PFC, insula) in all primary ROIs (see the “Results” section), we performed a follow-up voxelwise regression analysis to test if any subregions within the above-mentioned primary ROIs were driving these effects, again controlling for *TSPO* genotype. To this end, we used nonparametric permutation testing (randomize, FSL) with 10,000 permutations, 5 mm variance smoothing, threshold-free cluster enhancement, and a search volume restricted to include only the primary a priori ROIs. We then compared the PET signal from patients with little-to-no depression (BDI score = 0–9; $n = 18$) or mild-to-moderate depression (BDI score = 10–18; $n = 7$) against that from healthy, non-depressed controls, using ranges recommended in patients with medical illness for the BDI version used in the current study [53]. Using ANCOVAs, we compared mean [^{11}C]PBR28 SUVR, extracted from clusters significant in the voxelwise regression analysis (aMCC and pgACC), between these subgroups of patients and healthy, non-depressed controls (CTRL). Of note, because the primary aim of the study was to perform cross-sectional analyses within the patient group only, healthy controls were evaluated under different protocols, and were not specifically recruited to match the patients. Because group differences in injected dose and age reached or approached statistical significance (see the “Results” section), these variables were included, in addition to *TSPO* polymorphism, as regressors of no interest in our analyses. Because previous research in depressed patients demonstrated elevated TSPO PET signal compared with controls, and our own regression analyses in the patient group demonstrated a positive correlation between depression scores and TSPO PET signal, statistically significant group effects in the ANCOVA were

decomposed using one-sided Dunnett's post hoc pairwise comparisons to test the hypothesis that mean PET signal in the two subgroups of cLBP patients was higher than mean PET signal in healthy controls. The use of an ANCOVA was justified because the distribution of the residuals for all regions or any groups did not significantly vary from normality (p 's > 0.078, Shapiro-Wilk), and there were no violations of the equal variance assumption for either region (p 's > 0.48, Levene's test).

Next, we evaluated functional connectivity of the regions showing an association between PET signal and BDI scores in the voxelwise regression analysis, using resting-state fMRI data collected simultaneously to the PET data. First-level general linear model analyses were performed, modeling seed region time series as a regressor of interest, as well as the following nuisance regressors: six motion parameters (three translations, three rotations from FSL's *mcfliirt* tool), motion-flagged volumes (identified by *fsl_motion_outliers*), and the first five PCA components from CSF and WM [54]. The resulting connectivity maps were passed up to a second-level analysis, where they were regressed against the [^{11}C]PBR28 SUVR extracted from the same seed, in order to determine whether PET signal in a given region was associated with the functional connectivity between that brain region and others. These analyses were carried out with the nonparametric randomize tool, as described above. As the regions used as seeds in the connectivity analyses were selected because of their association between PET signal and BDI scores, we further hypothesized that any connectivity patterns identified as showing an association with the PET signal (pgACC to dorsolateral prefrontal cortex, pgACC-dlPFC; see the “Results” section) would also be associated with BDI scores. To test this hypothesis, mean pgACC-dlPFC z -scores were regressed against BDI. Finally, in order to gain a more mechanistic understanding of the relation between neuroinflammation, functional connectivity and depressive scores, we performed exploratory mediation analyses. Of all the possible model configurations, we elected to test only mediation models in which depressive symptoms were dependent on [^{11}C]PBR28 PET signal (but not vice versa), because inflammatory signaling is known to induce depressive behaviors in humans and animal models [55, 56]. As such, we designed three mediation models with the following independent, mediator and dependent variables (IV/M/DV): IV = connectivity, M = [^{11}C]PBR28 signal, DV = BDI (model 1); IV = [^{11}C]PBR28 signal, M = connectivity, DV = BDI (model 2); IV = [^{11}C]PBR28 signal, M = BDI, DV = connectivity (model 3). The unstandardized regression coefficients in this mediation model and the bootstrap 95% confidence intervals (CIs) for total and indirect effects of the independent variable on the dependent variable through M (1000 bootstrap samples) were estimated using

the Preacher and Hayes Indirect Mediation Analysis tool for SPSS [57], version 20 (IBM Corp, Armonk, NY). As recommended, the indirect (i.e., mediation) effect was considered statistically significant if the bias corrected 95% CI did not include zero.

Results

Subject characteristics

Patients reported significantly more back pain ($p < 0.001$) and higher BDI scores ($p < 0.001$) compared with controls. Patient BDI scores ranged from low to mild/moderate, and were not correlated with either MPQ score or current pain ratings (r 's < 0.145 ; p 's < 0.48). See Supplementary Table 1 for more details.

[¹¹C]PBR28 signal is associated with depressive symptoms

First, we performed a region-of-interest (ROI) partial correlation analysis to assess the association between BDI scores and [¹¹C]PBR28 SUVR in patients (Fig. 1). Prefrontal cortex (PFC), insula, and anterior cingulate cortex (ACC) were selected as a priori ROIs [25]. In these analysis, TSPO PET signal demonstrated a positive correlation with BDI scores that was statistically significant in the ACC ($r = 0.494$, $p = 0.042$, corrected), but not for insula ($r = 0.47$, $p = 0.06$, corrected) or PFC ($r = 0.44$; $p = 0.099$, corrected; Fig. 1), after correction for multiple comparisons. There were no significant associations between [¹¹C]PBR28 signal and BDI in control thalamic ROIs (regions we previously showed to exhibit elevated [¹¹C]PBR28 signal in cLBP patients, but not expected to be related to NA), even when explored uncorrected (r 's < 0.163 , p 's > 0.446). In cLBP

patients, clinical pain during the scan was not significantly correlated with BDI scores ($p = 0.263$), or [¹¹C]PBR28 PET signal in any of the three a priori ROIs (p 's > 0.14).

In agreement with the ROI analyses, which show the strongest association in the ACC region, two clusters within the boundaries of this anatomical label were the only ones reaching significance in a follow-up nonparametric voxel-wise permutation analysis: the pregenual anterior and the anterior middle cingulate cortices (pgACC and aMCC) (Fig. 2a, b). There were no regions showing significant negative correlations between BDI and TSPO PET signal.

After demonstrating a linear association between [¹¹C]PBR28 PET signal and BDI scores in the patients, we sought to test the hypothesis that the PET signal in patients with higher depression symptom scores was significantly elevated compared with an existing dataset of healthy, non-depressed volunteers (Supplementary Table 1). We split the patients into those with little-to-no depression or mild-to-moderate depression [53]. ANCOVA analyses revealed a significant Group effect on [¹¹C]PBR28 signal in both regions identified in the voxelwise analyses (aMCC: $p < 0.001$; pgACC: $p = 0.005$). Post hoc analyses indicated that this effect was driven by patients with mild-to-moderate depression, which showed elevated PET signal compared with controls (aMCC: difference, 0.11; 95% CI, 0.08 to 0.13; $p < 0.001$; pgACC: difference, 0.12; 95% CI, 0.09 to 0.16; $p = 0.003$), whereas the non-depressed patients did not (aMCC: difference, -0.03 ; 95% CI, -0.04 to -0.02 ; $p = 0.937$; pgACC: difference, -0.02 ; 95% CI, -0.03 to -0.01 ; $p = 0.868$; Fig. 2c).

Pregenual TSPO PET signal mediates the association between depressive symptoms and frontolimbic connectivity

Next, we used BOLD resting-state fMRI data collected simultaneously to the PET data to evaluate functional

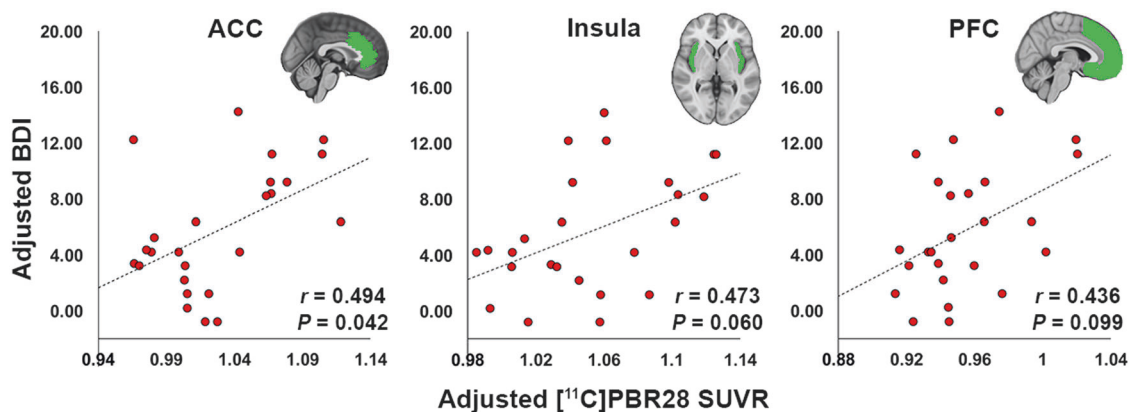
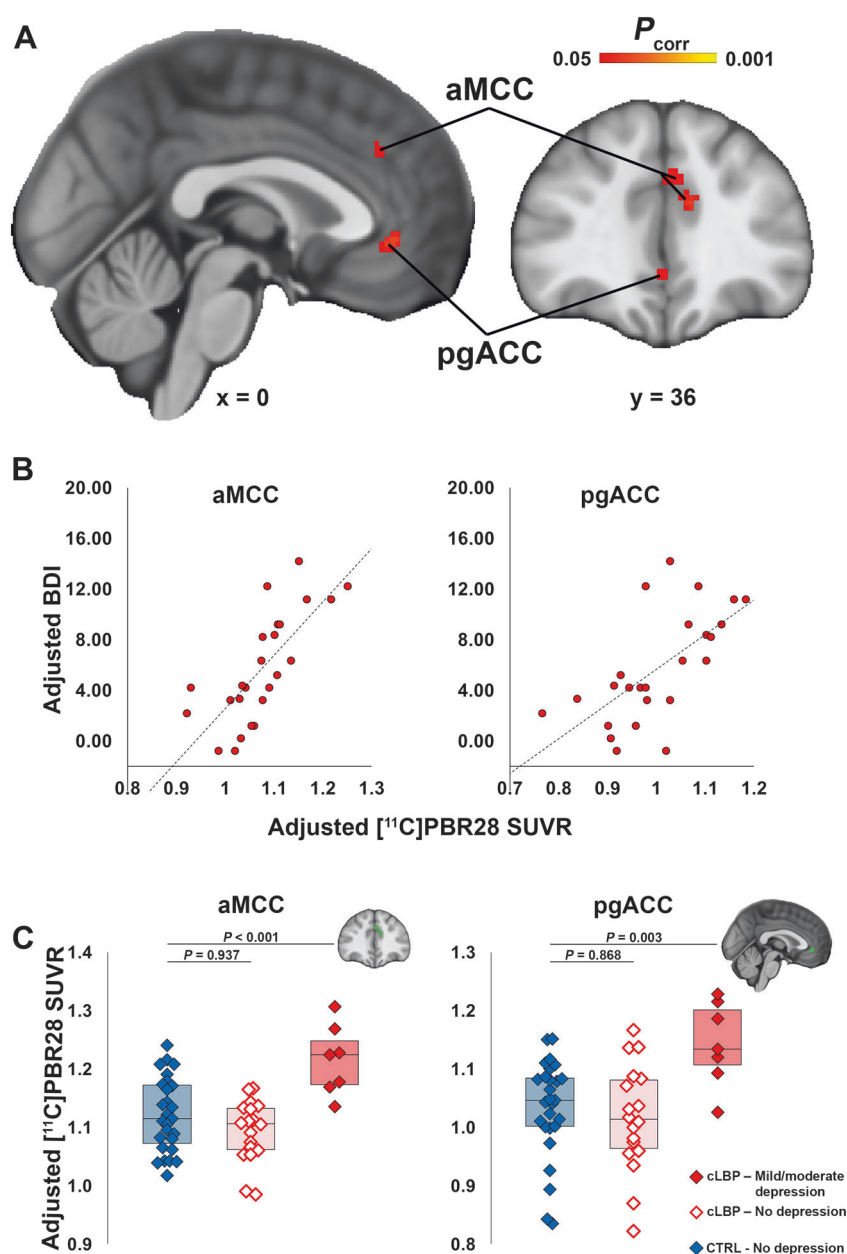


Fig. 1 ROI [¹¹C]PBR28 signal is associated with depressive symptoms. Scatterplots display the relationship between [¹¹C]PBR28 SUVR in each ROI (displayed in green) and BDI in cLBP patients ($n = 25$).

All data have been adjusted for TSPO polymorphism. BDI Beck Depression Inventory, ACC anterior cingulate cortex, PFC prefrontal cortex

Fig. 2 Voxelwise [^{11}C]PBR28 signal is associated with depressive symptoms and elevated in patients with mild-to-moderate depression. **a** Results from the voxelwise analysis showing clusters where [^{11}C]PBR28 SUVR is significantly positively associated with BDI. **b** For visualization purposes, average SUVR from the aMCC and pgACC clusters in panel (a) are plotted against BDI, both adjusted for *TSPO* polymorphism. **c** Results from the ANCOVA analysis comparing average aMCC and pgACC SUVR between cLBP patients with little-to-no depression, mild-to-moderate depression, and controls. *P*-values represent results from post-hoc Dunnett's tests comparing both patient subgroups against to controls. All values have been adjusted for age, injected dose, and *TSPO* polymorphism

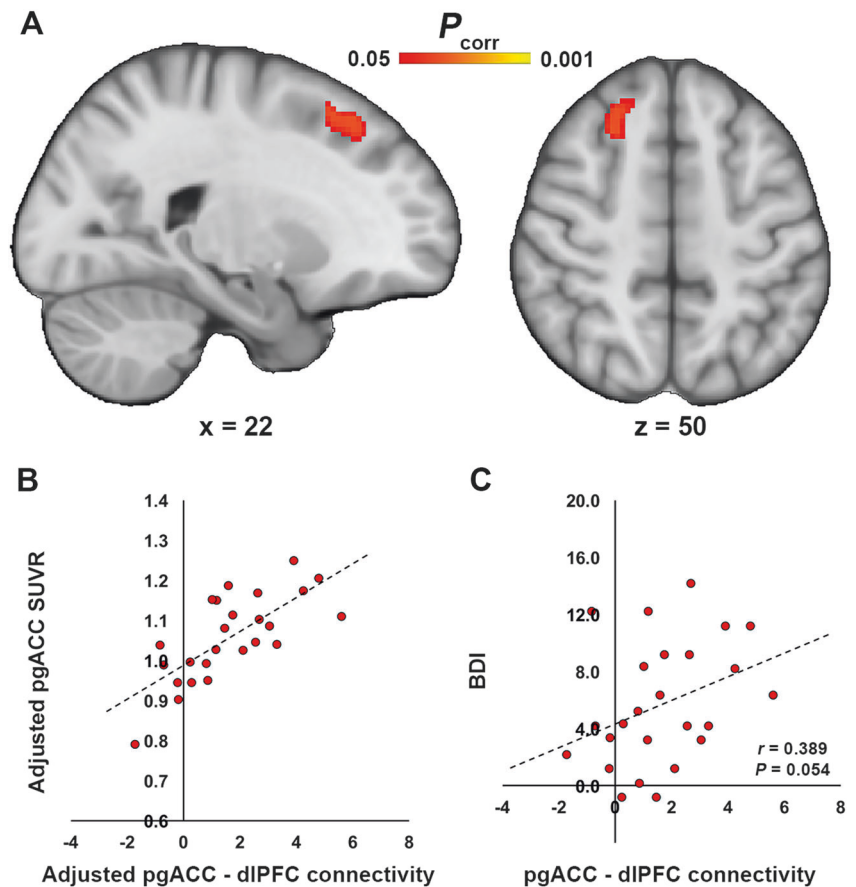


connectivity of the regions showing an association between PET signal and BDI scores in the voxelwise regression analysis. Using pgACC as a seed region, we observed that functional connectivity between the pgACC and dorsolateral PFC (dlPFC) was positively associated with pgACC [^{11}C]PBR28 signal (Fig. 3a, b). Average pgACC-dlPFC connectivity also showed a trend-level association with BDI ($p = 0.054$; Fig. 3c). *TSPO* PET signal in the aMCC was not significantly associated with aMCC functional connectivity.

Because of the observed intercorrelations between three variables of interest (BDI, pgACC [^{11}C]PBR28 signal, and pgACC-dlPFC connectivity), we conducted three exploratory bootstrapped mediation analyses to investigate whether

one variable was potentially mediating the relationship between the other two. Of these three models, only model 1 (IV, connectivity; M, [^{11}C]PBR28 PET signal; DV, BDI) reached statistical significance. This model revealed that the strength of the association between pgACC-dlPFC connectivity and BDI (path c; $\beta \pm$ standard error = 0.969 ± 0.48 , $p = 0.054$) was significantly reduced after accounting for the effects of the mediator, pgACC [^{11}C]PBR28 signal, (path c'; $\beta = -0.172 \pm 0.61$; $p = 0.780$). The bias corrected 95% CIs for the indirect effect of pgACC-dlPFC on BDI through pgACC SUVR (path a \times b; $\beta = 0.06 \pm 0.57$) yielded a lower limit of 0.352 and an upper limit of 2.57. A 95% CI range not containing zero suggests that pgACC [^{11}C]PBR28 signal significantly mediates the association

Fig. 3 Frontocingulate connectivity is associated with pgACC [¹¹C]PBR28 signal, and with BDI. **a** Results from the voxelwise nonparametric permutation analysis showing a significant positive association between pgACC [¹¹C]PBR28 SUVR and functional connectivity between pgACC and right dIPFC. **b** For visualization purposes, the average z-statistic was extracted from the dIPFC cluster in panel (a) and plotted against pgACC SUVR. All data have been adjusted for *TSPO* polymorphism. **c** A scatterplot shows the regression between average z-statistic connectivity extracted from dIPFC in panel (a) and BDI



between pgACC-dIPFC connectivity and BDI score (Fig. 4).

Discussion

Here, we show that [¹¹C]PBR28 PET signal in the pgACC is associated with frontolimbic connectivity and depressive symptoms, and mediates the relationship between the former and the latter, in chronic pain patients.

Because *TSPO* is upregulated by glial cells during neuroimmune activation [28], our observations agree with, and extend, results from a growing body of literature supporting a role for neuroinflammation in mood disorders, including both in vivo and in vitro studies. For example, postmortem studies in depressed or suicidal patients showed elevated inflammatory cytokine levels or markers of glial activation in ACC and PFC [58–61]. Preclinical studies have demonstrated brain microglial activation and increased neuroinflammatory markers in models of chronic stress [15–19] in regions consistent with those observed in the present study. In clinically depressed patients, brain *TSPO* PET binding was elevated compared with healthy volunteers [23–26], and positively correlated with depressive symptoms in the ACC, PFC, and insula [25]. Here, we have

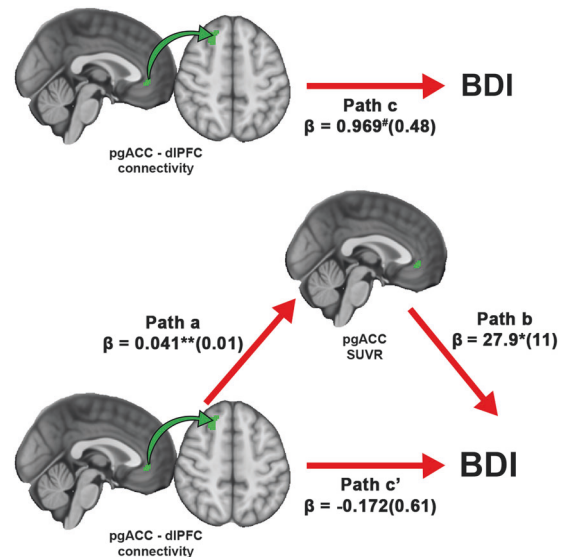


Fig. 4 pgACC [¹¹C]PBR28 signal mediates the relationship between pgACC-dIPFC connectivity and BDI. A bootstrapped mediation analysis revealed that pgACC significantly mediated the relationship between pgACC-dIPFC connectivity and BDI. Values within parentheses represent bootstrap standard errors for each path. #*p* = 0.054, **p* < 0.05, ***p* < 0.01

identified in the very same regions a positive association between [¹¹C]PBR28 signal and BDI scores, although

significantly only for the ACC after correction for multiple comparisons (with the PFC and insula being significant only at an uncorrected level). Interestingly, no such relationship was observed for the thalamus, a region demonstrating consistently elevated TSPO PET signal in cLBP patients compared with healthy controls in our previous work [21]. This observation suggests that different spatial patterns of glial activation may contribute independently to specific symptoms.

Our study further shows a relationship between pgACC [^{11}C]PBR28 PET signal and pgACC-dIPFC connectivity, a neural metric that previous fMRI research found to be positively correlated with negative self-focused thought in depressed patients [36]. The association between TSPO PET signal and functional connectivity could reflect different mechanisms. First, glial cells can modulate neuronal activity [62, 63], and might therefore play a role in dysfunctional neuronal communication in numerous pathologies [64], including depression [65]. Studies show that manipulation of fractalkine receptors, expressed only on microglia, is sufficient to alter synaptic function: fractalkine receptor activation releases pro-inflammatory cytokines and increases excitatory signaling [31], whereas attenuation of fractalkine signaling inhibits pro-inflammatory signaling [66]. Furthermore, fractalkine receptor knockout animals show deficient synaptic pruning during development, weakened synaptic transmission and reduced functional brain connectivity [67]. While these studies highlight the ability of glial cells to regulate neural activity in preclinical models, the results of our analyses suggest that connectivity may be instead driving neuroinflammation in our dataset. In our analyses, pgACC TSPO PET signal significantly mediated the relationship between pgACC-dIPFC connectivity and BDI. Importantly, the mediation model in which the directionality of the association between connectivity and PET signal was reversed (model 2) was not statistically significant. Therefore, our results lead us to speculate that changes in frontolimbic connectivity may cause NA indirectly, by exerting an effect on glial activation. As glial cells are sensitive to neural activity and can change activation states as a result of activity changes [32], it is possible that aberrant communication between the dIPFC and pgACC predates and contributes to neuroinflammation in the pgACC. While statistical modeling can provide hints at the possible neuroglial mechanisms leading to depressive symptoms, it is important to stress that causality cannot be conclusively demonstrated solely on the basis of the existing data, and specifically designed studies will be ultimately needed to provide empirical evidence corroborating our interpretation.

Several caveats should be considered when interpreting the results of our report. First, contributions of specific glial subtypes cannot be resolved with TSPO PET imaging. In

fact, while elevations in TSPO levels are most commonly interpreted as evidence of microglial activation, in some circumstances this protein can (also) be upregulated by reactive astrocytes [68, 69]. However, studies implicating astrocytic involvement in major depression [70] support a reduction, rather than an increase, in astrocytic density and expression of astrocytic markers. As such, it seems more likely that the depressive symptom-associated elevations in TSPO observed here are reflective of microglial activation. Moreover, we have recently shown that TSPO elevations observed in a different chronic pain disorder (fibromyalgia) are not accompanied by elevations in [^{11}C]-L-deprenyl- D_2 signal [71]. Because the latter is thought to reflect mostly astrocytic contributions [72], this observation suggests that microglia and not astrocytes might be driving the TSPO signal, although whether this conclusion can be generalized to cLBP awaits experimental verification. Second, the healthy volunteer data included in this study for secondary analyses came from an existing dataset of participants recruited through different protocols, and thus not specifically recruited to match these patients. As a result, the former happened to have a higher average injected dose and tended to be marginally older. However, neither injected mass nor specific activity were significantly different across groups, and increasing age is more likely to be associated with higher, rather than lower, TSPO signal [73–75]. Thus, we deem it unlikely that any of our results might be explained by the above-mentioned group differences. Perhaps most importantly, these group differences have no bearing on the main observation of the study, which is the association between PET signal and BDI in the cLBP group. Finally, in this study we used a simplified ratio metric (SUVR) as the primary outcome measure. Measures obtained with kinetic modeling using arterial input functions (e.g., distribution volume [V_T] and V_T ratio [DVR]) are still largely considered the gold standard for quantification of TSPO tracers. However, in a subset of the participants we were able to verify that SUVR was significantly correlated with DVR in all regions evaluated in this study (with the exception of the prefrontal ROI, which showed a strong trend; Supplementary Fig. 1), suggesting that this metric is an appropriate surrogate for TSPO quantification, at least in this population. In addition, the use of ratio metrics such as SUVR or DVR, instead of an absolute metric such as SUV or V_T , may come with drawbacks. Because no brain region devoid of TSPO exists, a true reference region cannot be identified, and the selection of the pseudoreference region to be used to normalize the signal relies on the assumption that that region is not affected by pathology. On the other hand, this approach can increase the sensitivity to detect neuroinflammatory responses as it can correct for the large interindividual variability in global signal often observed with TSPO tracers [48]. Indeed, our group and others have

used ratio metrics to demonstrate TSPO signal increases across multiple conditions, in spatial distributions overlapping with the known or expected distribution of neuroinflammation in each condition (e.g. motor/premotor cortices and corticospinal tracts in amyotrophic lateral sclerosis [43, 76]; basal ganglia in Huntington's disease [50], temporoparietal regions in Alzheimer's disease) [77].

In conclusion, the present results provide evidence supporting a role for glial activation in depressive symptoms comorbid with chronic pain and, more broadly, further corroborate the neuroinflammatory hypothesis of negative affect [25]. Our findings therefore support the exploration of neuroinflammation as a therapeutic target for conditions characterized by NA, including chronic pain.

Acknowledgements The authors would like to thank Grae Arabasz, Shiley Hsu, Regan Butterfield, Judit Sore, Patricia McCarthy, Marlene Wentworth, Amy Kendall, and Natacha Nortelus for help with data collection. They would like to thank Dr. Marc O. Martel for helpful discussions. The study was supported by the following funding sources: 1R21NS087472-01A1 (MLL), 1R01NS095937-01A1 (MLL), DoD-W81XWH-14-1-0543 (MLL), and 1R01NS094306-01A1 (MLL), Harvard Catalyst Advance Imaging Pilot Grant (JMH), 5T32EB13180 (T32 supporting DSA), P41RR14075, and P41EB015896.

Compliance with ethical standards

Conflict of interest The authors declare that they have no conflict of interest.

Publisher's note: Springer Nature remains neutral with regard to jurisdictional claims in published maps and institutional affiliations.

References

1. Leo RJ. Chronic pain and comorbid depression. *Curr Treat Options Neurol*. 2005;7:403–12.
2. Jamison RN, Edwards RR, Liu X, Ross EL, Michna E, Warnick M, et al. Relationship of negative affect and outcome of an opioid therapy trial among low back pain patients. *Pain Pract*. 2013;13:173–81.
3. Linton SJ. A review of psychological risk factors in back and neck pain. *Spine*. 2000;25:1148–56.
4. Pincus T, Burton AK, Vogel S, Field AP. A systematic review of psychological factors as predictors of chronicity/disability in prospective cohorts of low back pain. *Spine*. 2002;27:E109–120.
5. Wasan AD, Davar G, Jamison R. The association between negative affect and opioid analgesia in patients with discogenic low back pain. *Pain*. 2005;117:450–61.
6. Arnow BA, Hunkeler EM, Blasey CM, Lee J, Constantino MJ, Fireman B, et al. Comorbid depression, chronic pain, and disability in primary care. *Psychosom Med*. 2006;68:262–8.
7. Haythornthwaite JA, Sieber WJ, Kerns RD. Depression and the chronic pain experience. *Pain*. 1991;46:177–84.
8. Krause SJ, Wiener RL, Tait RC. Depression and pain behavior in patients with chronic pain. *Clin J Pain*. 1994;10:122–7.
9. Lopresti AL, Maker GL, Hood SD, Drummond PD. A review of peripheral biomarkers in major depression: the potential of inflammatory and oxidative stress biomarkers. *Prog Neuropsychopharmacol Biol Psychiatry*. 2014;48:102–11.
10. Walker AK, Kavelaars A, Heijnen CJ, Dantzer R. Neuroinflammation and comorbidity of pain and depression. *Pharmacol Rev*. 2014;66:80–101.
11. LeBlanc BW, Zerah ML, Kadasi LM, Chai N, Saab CY. Minocycline injection in the ventral posterolateral thalamus reverses microglial reactivity and thermal hyperalgesia secondary to sciatic neuropathy. *Neurosci Lett*. 2011;498:138–42.
12. Di Cesare Mannelli L, Pacini A, Bonaccini L, Zanardelli M, Mello T, Ghelardini C. Morphologic features and glial activation in rat oxaliplatin-dependent neuropathic pain. *J Pain*. 2013;14:1585–1600.
13. Miyamoto K, Kume K, Ohsawa M. Role of microglia in mechanical allodynia in the anterior cingulate cortex. *J Pharmacol Sci*. 2017;134:158–65.
14. Taylor AM, Mehrabani S, Liu S, Taylor AJ, Cahill CM. Topography of microglial activation in sensory- and affect-related brain regions in chronic pain. *J Neurosci Res*. 2017;95:1330–5.
15. Farooq RK, Isingrini E, Tanti A, Le Guisquet AM, Arlicot N, Minier F, et al. Is unpredictable chronic mild stress (UCMS) a reliable model to study depression-induced neuroinflammation? *Behav Brain Res*. 2012;231:130–7.
16. Hinwood M, Morandini J, Day TA, Walker FR. Evidence that microglia mediate the neurobiological effects of chronic psychological stress on the medial prefrontal cortex. *Cereb Cortex*. 2012;22:1442–54.
17. Tynan RJ, Naicker S, Hinwood M, Nalivaiko E, Buller KM, Pow DV, et al. Chronic stress alters the density and morphology of microglia in a subset of stress-responsive brain regions. *Brain Behav Immun*. 2010;24:1058–68.
18. Wohleb ES, Fenn AM, Pacenta AM, Powell ND, Sheridan JF, Godbout JP. Peripheral innate immune challenge exaggerated microglia activation, increased the number of inflammatory CNS macrophages, and prolonged social withdrawal in socially defeated mice. *Psychoneuroendocrinology*. 2012;37:1491–505.
19. Wohleb ES, Hanke ML, Corona AW, Powell ND, Stiner LM, Bailey MT, et al. beta-Adrenergic receptor antagonism prevents anxiety-like behavior and microglial reactivity induced by repeated social defeat. *J Neurosci*. 2011;31:6277–88.
20. Albrecht D, Ahmed S, Kettner N, Borra R, Cohen-Adad J, Deng H, et al. Neuroinflammation of the spinal cord and nerve roots in chronic radicular pain patients. *Pain*. 2018;159:968–77.
21. Loggia ML, Chonde DB, Akeju O, Arabasz G, Catana C, Edwards RR, et al. Evidence for brain glial activation in chronic pain patients. *Brain*. 2015;138(pt. 3):604–15.
22. Albrecht DS, Forsberg A, Sandstrom A, Bergan C, Kadetoff D, Protsenko E, et al. Brain glial activation in fibromyalgia—A multi-site positron emission tomography investigation. *Brain Behav Immun*. 2019;75:72–83.
23. Holmes SE, Hinz R, Conen S, Gregory CJ, Matthews JC, Anton-Rodriguez JM, et al. Elevated translocator protein in anterior cingulate in major depression and a role for inflammation in suicidal thinking: a positron emission tomography study. *Biological psychiatry*. 2018;83:61–69.
24. Setiawan E, Attwells S, Wilson AA, Mizrahi R, Rusjan PM, Miler L, et al. Association of translocator protein total distribution volume with duration of untreated major depressive disorder: a cross-sectional study. *Lancet Psychiatry*. 2018;5:339–47.
25. Setiawan E, Wilson AA, Mizrahi R, Rusjan PM, Miler L, Rajkowska G, et al. Role of translocator protein density, a marker of neuroinflammation, in the brain during major depressive episodes. *JAMA Psychiatry*. 2015;72:268–75.
26. Li H, Sagar AP, Keri S. Translocator protein (18kDa TSPO) binding, a marker of microglia, is reduced in major depression

- during cognitive-behavioral therapy. *Prog Neuropsychopharmacol Biol Psychiatr.* 2018;83:1–7.
27. Hannestad J, DellaGioia N, Gallezot JD, Lim K, Nabulsi N, Esterlis I, et al. The neuroinflammation marker translocator protein is not elevated in individuals with mild-to-moderate depression: a [(11)C]PBR28 PET study. *Brain Behav Immun.* 2013;33:131–8.
 28. Cagnin A, Kassiou M, Meikle SR, Banati RB. Positron emission tomography imaging of neuroinflammation. *Neurotherapeutics.* 2007;4:443–52.
 29. Cosenza-Nashat M, Zhao ML, Suh HS, Morgan J, Natividad R, Morgello S, et al. Expression of the translocator protein of 18 kDa by microglia, macrophages and astrocytes based on immunohistochemical localization in abnormal human brain. *Neuropathol Appl Neurobiol.* 2009;35:306–28.
 30. Rupprecht R, Papadopoulos V, Rammes G, Baghai TC, Fan J, Akula N, et al. Translocator protein (18 kDa) (TSPO) as a therapeutic target for neurological and psychiatric disorders. *Nat Rev Drug Discov.* 2010;9:971–88.
 31. Clark AK, Gruber-Schoffnegger D, Drdla-Schutting R, Gerhold KJ, Malcangio M, Sandkuhler J. Selective activation of microglia facilitates synaptic strength. *J Neurosci.* 2015;35:4552–70.
 32. Xanthos DN, Sandkuhler J. Neurogenic neuroinflammation: inflammatory CNS reactions in response to neuronal activity. *Nat Rev Neurosci.* 2014;15:43–53.
 33. Baliki MN, Petre B, Torbey S, Herrmann KM, Huang L, Schnitzer TJ, et al. Corticostriatal functional connectivity predicts transition to chronic back pain. *Nat Neurosci.* 2012;15:1117–9.
 34. Loggia ML, Kim J, Gollub RL, Vangel MG, Kirsch I, Kong J, et al. Default mode network connectivity encodes clinical pain: an arterial spin labeling study. *Pain.* 2013;154:24–33.
 35. Greicius MD, Flores BH, Menon V, Glover GH, Solvason HB, Kenna H, et al. Resting-state functional connectivity in major depression: abnormally increased contributions from subgenual cingulate cortex and thalamus. *Biol Psychiatry.* 2007;62:429–37.
 36. Philippi CL, Cornejo MD, Frost CP, Walsh EC, Hoks RM, Birn R, et al. Neural and behavioral correlates of negative self-focused thought associated with depression. *Hum Brain Mapp.* 2018;39:2246–57.
 37. Kreisl WC, Jenko KJ, Hines CS, Lyoo CH, Corona W, Morse CL, et al. A genetic polymorphism for translocator protein 18 kDa affects both in vitro and in vivo radioligand binding in human brain to this putative biomarker of neuroinflammation. *J Cereb Blood Flow Metab.* 2013;33:53–58.
 38. Owen DR, Yeo AJ, Gunn RN, Song K, Wadsworth G, Lewis A, et al. An 18-kDa translocator protein (TSPO) polymorphism explains differences in binding affinity of the PET radioligand PBR28. *J Cereb Blood Flow Metab.* 2012;32:1–5.
 39. Beck AT, Ward CH, Mendelson M, Mock J, Erbaugh J. An inventory for measuring depression. *Arch Gen Psychiatry.* 1961;4:561–71.
 40. Geisser ME, Roth RS, Robinson ME. Assessing depression among persons with chronic pain using the Center for Epidemiological Studies-Depression Scale and the Beck Depression Inventory: a comparative analysis. *Clin J Pain.* 1997;13:163–70.
 41. Melzack R. The short-form McGill Pain Questionnaire. *Pain.* 1987;30:191–7.
 42. Albrecht DS, Normandin MD, Shcherbinin S, Wooten DW, Schwarz AJ, Zurcher NR et al. Pseudo-reference regions for glial imaging with (11)C-PBR28: investigation in two clinical cohorts. *J Nucl Med.* 2017;59:107–14.
 43. Zurcher NR, Loggia ML, Lawson R, Chonde DB, Izquierdo-Garcia D, Yasek JE, et al. Increased in vivo glial activation in patients with amyotrophic lateral sclerosis: assessed with [(11)C]-PBR28. *Neuroimage Clin.* 2015;7:409–14.
 44. Kolb A, Wehrl HF, Hofmann M, Judenhofer MS, Eriksson L, Ladebeck R, et al. Technical performance evaluation of a human brain PET/MRI system. *Eur Radiol.* 2012;22:1776–88.
 45. Imaizumi M, Kim HJ, Zoghbi SS, Briard E, Hong J, Musachio JL, et al. PET imaging with [(11)C]PBR28 can localize and quantify upregulated peripheral benzodiazepine receptors associated with cerebral ischemia in rat. *Neurosci Lett.* 2007;411:200–5.
 46. Izquierdo-Garcia D, Hansen AE, Forster S, Benoit D, Schachoff S, Furst S, et al. An SPM8-based approach for attenuation correction combining segmentation and nonrigid template formation: application to simultaneous PET/MR brain imaging. *J Nucl Med.* 2014;55:1825–30.
 47. Coughlin JM, Wang Y, Munro CA, Ma S, Yue C, Chen S, et al. Neuroinflammation and brain atrophy in former NFL players: an in vivo multimodal imaging pilot study. *Neurobiol Dis.* 2015;74:58–65.
 48. Turkheimer FE, Rizzo G, Bloomfield PS, Howes O, Zanotti-Fregonara P, Bertoldo A, et al. The methodology of TSPO imaging with positron emission tomography. *Biochem Soc Trans.* 2015;43:586–92.
 49. Vera JH, Guo Q, Cole JH, Boasso A, Greathead L, Kelleher P, et al. Neuroinflammation in treated HIV-positive individuals: a TSPO PET study. *Neurology.* 2016;86:1425–32.
 50. Lois C, Gonzalez I, Izquierdo-Garcia D, Zurcher NR, Wilkens P, Loggia ML, et al. Neuroinflammation in Huntington's Disease: New Insights with (11)C-PBR28 PET/MRI. *ACS Chem Neurosci.* 2018;9:2563–71.
 51. Behzadi Y, Restom K, Liu J, Liu TT. A component based noise correction method (CompCor) for BOLD and perfusion based fMRI. *Neuroimage.* 2007;37:90–101.
 52. Yarkoni T, Poldrack RA, Nichols TE, Van Essen DC, Wager TD. Large-scale automated synthesis of human functional neuroimaging data. *Nat Methods.* 2011;8:665–70.
 53. Beck AT, Steer RA, Carbin MG. Psychometric properties of the Beck Depression Inventory: Twenty-five years of evaluation. *Clin Psychol Rev.* 1988;8:77–100.
 54. Chai XJ, Castanon AN, Ongur D, Whitfield-Gabrieli S. Anticorrelations in resting state networks without global signal regression. *Neuroimage.* 2012;59:1420–8.
 55. Dantzer R, O'Connor JC, Freund GG, Johnson RW, Kelley KW. From inflammation to sickness and depression: when the immune system subjugates the brain. *Nat Rev Neurosci.* 2008;9:46–56.
 56. Sandiego CM, Gallezot JD, Pittman B, Nabulsi N, Lim K, Lin SF, et al. Imaging robust microglial activation after lipopolysaccharide administration in humans with PET. *Proc Natl Acad Sci USA.* 2015;112:12468–73.
 57. Preacher KJ, Hayes AF. Asymptotic and resampling strategies for assessing and comparing indirect effects in multiple mediator models. *Behav Res Methods.* 2008;40:879–91.
 58. Dean B, Tawadros N, Scarr E, Gibbons AS. Regionally-specific changes in levels of tumour necrosis factor in the dorsolateral prefrontal cortex obtained postmortem from subjects with major depressive disorder. *J Affect Disord.* 2010;120:245–8.
 59. Pandey GN, Rizavi HS, Ren X, Fareed J, Hoppensteadt DA, Roberts RC, et al. Proinflammatory cytokines in the prefrontal cortex of teenage suicide victims. *J Psychiatr Res.* 2012;46:57–63.
 60. Steiner J, Walter M, Gos T, Guillemin GJ, Bernstein HG, Samyay Z, et al. Severe depression is associated with increased microglial quinolinic acid in subregions of the anterior cingulate gyrus: evidence for an immune-modulated glutamatergic neurotransmission? *J Neuroinflammation.* 2011;8:94.
 61. Torres-Platas SG, Cruceanu C, Chen GG, Turecki G, Mechawar N. Evidence for increased microglial priming and macrophage recruitment in the dorsal anterior cingulate white matter of depressed suicides. *Brain Behav Immun.* 2014;42:50–59.

62. Ren K, Dubner R. Activity-triggered tetrapartite neuron-glia interactions following peripheral injury. *Curr Opin Pharmacol*. 2016;26:16–25.
63. Wu Y, Dissing-Olesen L, MacVicar BA, Stevens B. Microglia: Dynamic Mediators of Synapse Development and Plasticity. *Trends Immunol*. 2015;36:605–13.
64. Nistico R, Salter E, Nicolas C, Feligioni M, Mango D, Bortolotto ZA, et al. Synptoimmunology—roles in health and disease. *Mol Brain*. 2017;10:26.
65. Rial D, Lemos C, Pinheiro H, Duarte JM, Goncalves FQ, Real JI, et al. Depression as a glial-based synaptic dysfunction. *Front Cell Neurosci*. 2015;9:521.
66. Freria CM, Hall JC, Wei P, Guan Z, McTigue DM, Popovich PG. Deletion of the fractalkine receptor, CX3CR1, improves endogenous repair, axon sprouting, and synaptogenesis after spinal cord injury in mice. *J Neurosci*. 2017;37:3568–87.
67. Zhan Y, Paolicelli RC, Sforazzini F, Weinhard L, Bolasco G, Pagani F, et al. Deficient neuron-microglia signaling results in impaired functional brain connectivity and social behavior. *Nature Neurosci*. 2014;17:400–6.
68. Liu X, Liu H, Xu S, Tang Z, Xia W, Cheng Z, et al. Spinal translocator protein alleviates chronic neuropathic pain behavior and modulates spinal astrocyte-neuronal function in rats with L5 spinal nerve ligation model. *Pain*. 2016;157:103–16.
69. Wei XH, Wei X, Chen FY, Zang Y, Xin WJ, Pang RP, et al. The upregulation of translocator protein (18 kDa) promotes recovery from neuropathic pain in rats. *J Neurosci*. 2013;33:1540–51.
70. Rajkowska G, Stockmeier CA. Astrocyte pathology in major depressive disorder: insights from human postmortem brain tissue. *Curr Drug Targets*. 2013;14:1225–36.
71. Albrecht DS, Forsberg A, Sandstrom A, Bergan C, Kadetoff D, Protsenko E, et al. Brain glial activation in fibromyalgia—a multi-site positron emission tomography investigation. *Brain Behav Immun*. 2019;75:72–83.
72. Ekblom J, Jossan SS, Orelund L, Walum E, Aquilonius SM. Reactive gliosis and monoamine oxidase B. *J Neural Transm Suppl*. 1994;41:253–8.
73. Gulyas B, Vas A, Toth M, Takano A, Varrone A, Cselenyi Z, et al. Age and disease related changes in the translocator protein (TSPO) system in the human brain: positron emission tomography measurements with [11C]vinpocetine. *Neuroimage*. 2011;56:1111–21.
74. Kumar A, Muzik O, Shandal V, Chugani D, Chakraborty P, Chugani HT. Evaluation of age-related changes in translocator protein (TSPO) in human brain using (11)C-[R]-PK11195 PET. *J Neuroinflammation*. 2012;9:232.
75. Paul S, Gallagher E, Liow JS, Mabins S, Henry K, Zoghbi SS, et al. Building a database for brain 18 kDa translocator protein imaged using [(11)C]PBR28 in healthy subjects. *J Cereb Blood Flow Metab*. 2018. <https://doi.org/10.1177/0271678X18771250>. [Epub ahead of print].
76. Alshikho MJ, Zurcher NR, Loggia ML, Cernasov P, Reynolds B, Pijanowski O, et al. Integrated magnetic resonance imaging and [(11) C]-PBR28 positron emission tomographic imaging in amyotrophic lateral sclerosis. *Annal Neurol*. 2018;83:1186–97.
77. Lyoo CH, Ikawa M, Liow JS, Zoghbi SS, Morse CL, Pike VW, et al. Cerebellum can serve as a pseudo-reference region in Alzheimer disease to detect neuroinflammation measured with PET radioligand binding to translocator protein. *J Nucl Med*. 2015;56:701–6.